

Primary and secondary red bed magnetization constrained by fluvial intraclasts

Nicholas L. Swanson-Hysell¹, Luke M. Fairchild¹, Sarah P. Slotznick¹

¹Department of Earth and Planetary Science, University of California, Berkeley, CA, USA

Key Points:

- Red siltstone intraclasts within a 1.1-billion-year-old formation reveal two ancient magnetization held by hematite – one acquired before redeposition of the clasts in the sedimentary environment and the other after burial.
- The fine-grained population of post-depositional hematite spans the superparamagnetic to single domain transition leading to a wide range of thermal unblocking temperatures. The coarser detrital population thermally unblocks in a narrower and higher temperature range.
- Thermal demagnetization can isolate the detrital and chemical remanence if conducted at very high-resolution close the Néel temperature of hematite

15 **Abstract**

16 The magnetization of hematite-bearing sedimentary rocks provides critical records of ge-
 17 omagnetic reversals and paleogeography. However, the timing of hematite remanent mag-
 18 netization acquisition is typically difficult to constrain and has led to much controversy
 19 in the interpretation of such data. This so-called “red bed controversy” stems from the
 20 reality that while detrital hematite in sediment can lead to a primary depositional re-
 21 manent magnetization, alteration of minerals through interaction with oxygen can lead
 22 to the post-depositional formation of hematite. Growth of hematite crystals within sed-
 23 iments could occur in a geologically short time period immediately following deposition
 24 or could occur thousands to millions of years later due to the passage of oxygenated flu-
 25 ids following burial. Given that many paleomagnetic field tests such as the reversal test
 26 and fold test could still “pass” in scenarios with secondary post-depositional hematite
 27 growth, this problem has been particularly intractable in many sedimentary successions.
 28 In this study, we use exceptionally well-preserved fluvial sediments within the 1.1 billion-
 29 year-old Freda Formation to gain insight into the timing of hematite remanence acqui-
 30 sition. This deposit contains siltstone intraclasts that were eroded from a coexisting litho-
 31 facies and redeposited within channel sandstone. Thermal demagnetization and petro-
 32 graphic data from these clasts reveal that they contain two generations of hematite. One
 33 population of hematite demagnetized at the highest unblocking temperatures and records
 34 directions that rotated along with the rip-up clasts. This component is a primary de-
 35 trital remanent magnetization that formed prior to the reorientation of the clasts within
 36 the river. The other component is removed at lower unblocking temperatures and has
 37 a consistent direction throughout the intraclasts. This component is held by a popula-
 38 tion of finer-grained hematite that grew and acquired a chemical remanent magnetiza-
 39 tion following deposition. The data support the interpretation that the magnetization
 40 of hematite-bearing sedimentary rocks held by >400 nm grains is more likely to record
 41 magnetization from the time of deposition and can be successfully isolated from co-occurring
 42 authigenic hematite through high-resolution thermal demagnetization.

43 **1 Introduction**

44 The magnetizations of hematite-bearing sedimentary rocks known as “red beds”
 45 have provided ample opportunities for Earth scientists to gain insight into the ancient
 46 geomagnetic field and the paleogeographic positions of sedimentary basins. However, with
 47 these opportunities has come much scientific debate, leading to what has been referred
 48 to as the “red bed controversy” (Beck, Burmester, & Housen, 2003; Butler, 1992; Van
 49 Der Voo & Torsvik, 2012). This controversy stems from the reality that hematite within
 50 sedimentary rocks can have two sources: 1) detrital grains that are within the sediment
 51 at the time of deposition; 2) grains that grow *in situ* after the sediments have been de-
 52 posited.

53 How does one constrain the relative age of hematite within sedimentary rocks? Many
 54 of the traditional paleomagnetic field tests are unable to differentiate between primary
 55 versus diagenetic remanence. For example, a structural fold test can constrain that a re-
 56 manence direction was obtained prior to folding, but millions of years have typically passed
 57 between the deposition of a sediment, its burial in a sedimentary basin, and such tec-
 58 tonic tilting. Dual polarity directions through a sedimentary succession are commonly
 59 interpreted as providing assurance that the remanence records primary or near-primary
 60 magnetization; however, hematite growth could occur significantly after deposition dur-
 61 ing a period when the geomagnetic field was reversing. Petrographic investigations are
 62 valuable, but it can be difficult to ascertain how much the petrographically observed hematite
 63 contributes to the magnetization and to unambiguously interpret whether observed grains
 64 are detrital or not (e.g. Elmore & Van der Voo, 1982). A common approach to classify
 65 hematite grains within red beds is into a fine-grained pigmentary population, typically
 66 interpreted to have formed within the sediment, and a coarser-grained population that

has been referred to in the literature as “specularite” (Butler, 1992; Van Der Voo & Torsvik, 2012). Tauxe, Kent, and Opdyke (1980) showed that sediments with abundant red pigmentary hematite in the Miocene Siwalik Group had lower thermal unblocking temperatures than grey samples dominated by a coarser-grained phase of specular hematite. An additional approach taken by Tauxe et al. (1980), and other workers going back to the work of Collinson (1965), is to seek to preferentially remove fine-grained pigmentary hematite through prolonged immersion in concentrated HCl acid. Paired chemical and thermal demagnetization have been interpreted to show that removal of pigmentary hematite coincides with lower unblocking temperatures supporting the interpretation that the coarser grains, that are more resistant to dissolution in acid, correspond with those that carry remanence removed at the highest unblocking temperatures (Bilardello & Kodama, 2010; Tauxe et al., 1980). Observations such as these have led to the practice of defining the characteristic remanent magnetization from hematite-bearing sediments as that held by the highest unblocking temperatures (Van Der Voo & Torsvik, 2012). Additional lines of evidence in numerous successions have supported this approach. For example, in the well-studied Carboniferous Mauch Chunk Formation of Pennsylvania, remanence removed up to $\sim 660^{\circ}\text{C}$ has uniform polarity while the component removed between upwards of 670°C is dual-polarity, was acquired before folding and is interpreted as a primary magnetization (DiVenere & Opdyke, 1991). Nevertheless, the primary versus secondary nature of micron-scale “specularite” grains that likely carry this remanence has been one of the largest sources of contention in the “red bed controversy” (Butler, 1992; Tauxe et al., 1980; Van Der Voo & Torsvik, 2012; Van Houten, 1968).

What is needed to most confidently address the timing of remanence acquisition is a process that reorients the sediment before it has been lithified. Two such processes that can occur within a siliciclastic depositional environment and be preserved in the rock record are: 1) syn-sedimentary slumping wherein coherent sediment is reoriented through soft-sediment folding in the surface environment and 2) intraclasts comprised of the lithology of interest that have been redeposited within the depositional environment. Sediments that have undergone reorienting sedimentary processes can provide significant insight into whether magnetization was acquired before or after reorientation.

Tauxe et al. (1980) studied 7 cobble-sized clasts within the Siwalik Group that were interpreted to have formed by cut-bank collapse and discovered that their magnetic remanence was acquired prior to clast reorientation. An investigation by Purucker, Elston, and Shoemaker (1980) on red beds of the Triassic Moenkopi Formation of Arizona used multiple such processes to gain insight into hematite acquisition. In their study, an intraformational landslide deposit with isoclinal folds of hematite-bearing claystone revealed non-uniform directions upon blanket demagnetization to 650°C that cluster better when corrected for their tilt, leading to a primary interpretation. Scatter was also observed in intraformational conglomerate clasts weathered out of an underlying unit upon blanket thermal demagnetization to 630°C . However, the lack of principal component analysis makes it difficult to evaluate the coherency of the directions. Complicating matters, Larson and Walker (1982) analyzed shale rip-up clasts in the same Moenkopi Formation and used the fact that similar remanence directions were removed between clasts during thermal demagnetization up to 645°C as support for the hypothesis that red beds rarely reflect the geomagnetic field at the time of deposition. Evaluating the robustness of this result is hindered by the cessation of thermal demagnetization before the Néel temperature of hematite and the lack of principal component analysis. These limitations are found in many studies from this era of research, when the red bed controversy was particularly fervent, as the work predates the widespread application of principal component analysis in conjunction with systematic progressive thermal demagnetization (Kirschvink, 1980; Van Der Voo & Torsvik, 2012).

In this study, we investigate cm-scale siltstone intraclasts within the Freda Formation that were eroded by fluvial processes and redeposited amongst cross-stratified sand-

120 stones (Fig. 1). High-resolution thermal demagnetization data on these clasts constrain
 121 the timing of hematite acquisition by revealing a primary component that formed prior
 122 to the erosion of the clasts within the depositional environment and a secondary com-
 123 ponent that formed following their redeposition.

124 The ~4 km thick Freda Formation was deposited in the Midcontinent Rift as it was
 125 thermally subsiding following the cessation of widespread magmatic activity (Cannon
 126 & Hinze, 1992). The fluvial sediments of the Freda Formation are part of the Orono Group
 127 and were deposited following the deposition of the alluvial Copper Harbor Conglomer-
 128 ate and the lacustrine Nonesuch Formation (Ojakangas, Morey, & Green, 2001). Abun-
 129 dant fine-grained red siltstones within the formation have a well-behaved magnetic re-
 130 manence dominated by hematite (Henry, Mauk, & Van der Voo, 1977). A maximum age
 131 constraint on the Freda Formation of $1085.57 \pm 0.25/1.3$ Ma (2σ analytical/analytical+tracer+decay
 132 constant uncertainty; Fairchild, Swanson-Hysell, Ramezani, Sprain, & Bowring, 2017)
 133 is provided by an U-Pb date of a lava flow within the underlying Copper Harbor Con-
 134 glomerate. Within the Freda Formation on the Keweenaw Peninsula are minor volcanics
 135 which are unlikely to be substantially younger than the youngest dated volcanics within
 136 the Midcontinent basin ($1083.52 \pm 0.23/1.2$ Ma from the Michipicoten Island Forma-
 137 tion; Fairchild et al., 2017). An age of ca. 1080 Ma for the basal 500 meters of the Freda
 138 Formation is consistent with modeling of post-rift thermal subsidence (Hutchinson, White,
 139 Cannon, & Schulz, 1990).

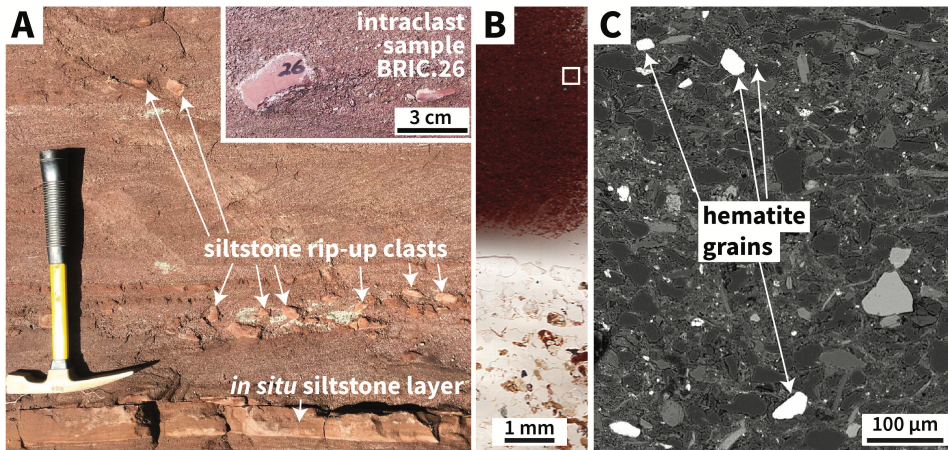


Figure 1. A: Siltstone intraclasts within the Freda Formation. The field photo shows an intact layer of siltstone below the hammer head which is topped by a bed of trough cross-stratified coarse sandstone with horizons of siltstone intraclasts. The hammer is 40 cm long. The inset photo is of an individual intraclast that was sampled as BRIC.26. B: A scan of a thin section of the BRIC.26 intraclast (upper half of image) and the coarse sand matrix (lower half of image). The red color of the intraclast is due to pigmentary hematite. C: Backscatter electron image of the siltstone clast from the region of the white box in B. The light-colored detrital grains (light due to iron's high atomic number) labeled with arrows were confirmed to be hematite through electron backscatter diffraction¹.

140 The studied outcrop is located along the Bad River (northern Wisconsin) in the
 141 lower portion of the Freda Formation – approximately 400 meters above its conformable
 142 base with the Nonesuch Formation. The two main lithofacies in the studied outcrop are:
 143 (1) siltstone to very fine sandstone with planar lamination and horizons of ripple cross-
 144 stratification and (2) coarse to very coarse subarkosic sandstone with dune-scale trough
 cross-stratification (Fig. 1). These lithofacies are consistent with a fluvial depositional

environment where the coarse sandstone facies are channel deposits and the siltstones are inner-bank or over-bank deposits. The coarse-grained sandstone contains horizons of tabular cm-scale intraclasts comprised of the dark red siltstone lithology that is present in underlying beds of intact siltstone (Fig. 1). These tabular clayey-silt intraclasts were eroded within the depositional environment and redeposited in the sandstone. Due to migrating channels in fluvial systems, it is expected for a river to erode its own sediments. The intraclasts would have been held together through cohesion resulting from the clay component within the sediment. Given that the clasts are large (1 to 7 cm) relative to their host sediment, that they are angular, and that they would have been fragile at the time of deposition, it is unlikely that they were transported far.

Paleomagnetic Results

Oriented samples were collected and analyzed from 39 Freda Formation intraclasts. The dimensions of the sampled clasts range from 2.2 x 1.4 x 0.5 cm to 7.2 x 2.3 x 1.2 cm. Given that the clasts were typically smaller than the 1-inch-diameter drill cores used for sampling, they were collected along with their sandstone matrix. These oriented cores were mounted onto quartz glass discs with Omega CC cement and the matrix material was micro-drilled away. The mounted clasts underwent stepwise thermal demagnetization in the UC Berkeley Paleomagnetism Lab using an ASC demagnetizer (residual fields <10 nT) with measurements made on a 2G DC-SQUID magnetometer. The demagnetization protocol had high resolution (5°C to 2°C to 1°C) approaching the Néel temperature of hematite resulting in 30 total thermal demagnetization steps (Fig. 2). All paleomagnetic data are available to the measurement level in the MagIC database (<https://earthref.org/MagIC/doi/>). So that reviewers have access to the data, they are currently available in CIT lab format and MagIC format here: https://github.com/Swanson-Hysell-Group/2018_Red_Bed_Intraclasts.

The clasts typically reveal two distinct magnetization directions. One direction was similar throughout the intraclasts and was typically removed between 200°C and 650°C (Fig. 2). This mid-temperature component is continuously unblocked between these temperatures with no or minimal downward inflection at ~580°C that would indicate remanence associated with magnetite (Fig. 2). This component is directionally well-grouped indicating that it was acquired following deposition of the clasts (Fig. 2). The other component trends towards the origin and is removed by thermal demagnetization steps at the highest levels such that it typically can be fit by a least-square line between 665°C and 688°C. The relative magnitude of the components varies between intraclasts (Fig. 2). While the high-temperature component can sometimes be fit as a line with a lower temperature bound of 660°C (BRIC.31a in Fig. 2), due to overlapping unblocking temperatures between the mid-temperature and high-temperature components the lower bounds of the high-temperature fits sometimes need to be as high as 680°C (BRIC.41a in Fig. 2). Note that while the Néel temperature of hematite is sometimes given as 675°C in the paleomagnetic literature, experimental data often show the Néel temperature to be as high as 690°C (Özdemir & Dunlop, 2006). There is typically a significant directional change in the specimen magnetization between the mid-temperature component and the high-temperature component (Fig. 2). As a result, 29 of the 39 analyzed intraclast specimens could be fit with distinct mid-temperature and high-temperature least-squares lines. An additional five specimens were undergoing directional change through the highest thermal demagnetization steps indicative of the presence of a distinct high-temperature component, but this component was not well-expressed enough to be fit. Five of the specimens showed no directional change and could be fit with a single mid-high-temperature component that is grouped with the mid-temperature component. In contrast to the well-grouped mid-temperature component, the high-temperature component directions are dispersed, indicating that the component was acquired prior to erosion and redeposition of the clasts. The high-temperature component directions are more dispersed in decli-

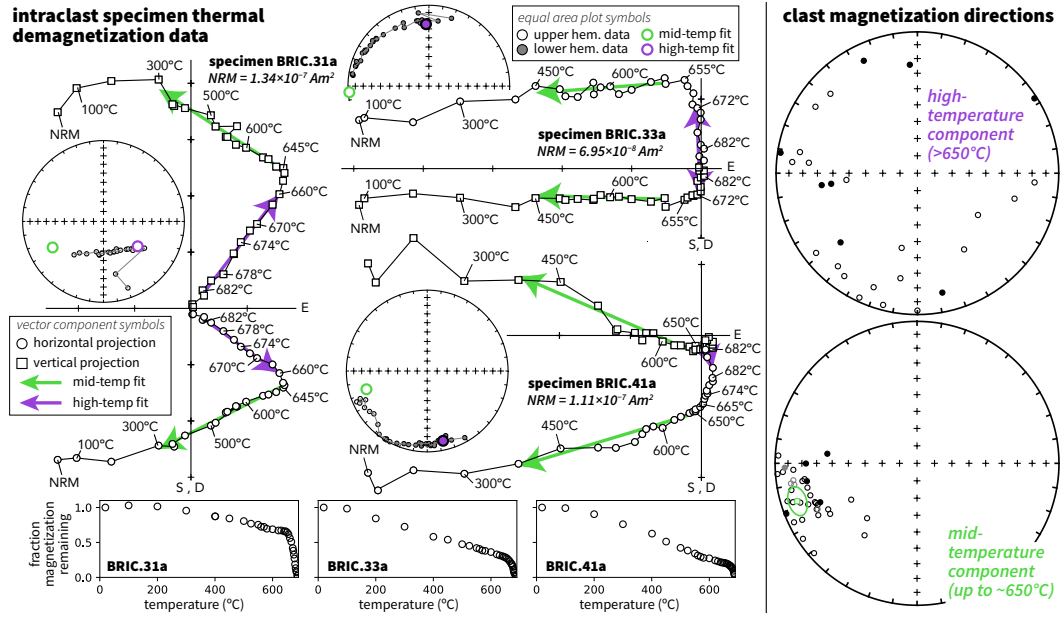


Figure 2. Paleomagnetic data from intraclasts reveal a mid-temperature component that typically unblocks prior to 655°C and a high-temperature component that typically unblocks between 655°C and 687°C. These components are present as varying fractions of the overall remanence as seen in the three individual clasts for which data are shown on vector component plots and measurement-level equal area plots in tilt-corrected coordinates (developed using PmagPy; Tauxe et al., 2016). The direction of the mid-temperature component is shown as purple arrows on the vector component plots and purple circles on the equal area plots while the high-temperature component is shown with green symbols. The mid-temperature component has a similar direction throughout the clasts as can be seen on the component directions equal area plots (mean declination: 252.4, inclination: -12.5, α_{95} : 6.6). In contrast, the high-temperature component directions are dispersed.

nation than inclination leading to a distribution that is not randomly dispersed on a sphere. Given that the clasts are tabular and were liberated along their depositional lamination and subsequently landed roughly bedding-parallel, it is to be expected that the rotations were largely around a vertical axis which would preferentially change declination.

202 Petrographic Results

Petrography on the intraclasts reveals two distinct populations of hematite (Fig. 1). One population is fine-grained pigmentary hematite present dominantly within the clay-sized matrix and rimming detrital silt-sized grains. The zones of pigmentary hematite within the matrix remain cloudy to high magnification indicating that the grains are sub-micron in size. The other population of hematite has similar sizes and shapes to other detrital silt-sized grains – typically ranging from 2 to 50 μm in diameter. These hematite grains were identified through reflected light microscopy with their mineralogy supported by energy-dispersive x-ray spectroscopy and confirmed by electron backscatter diffraction.

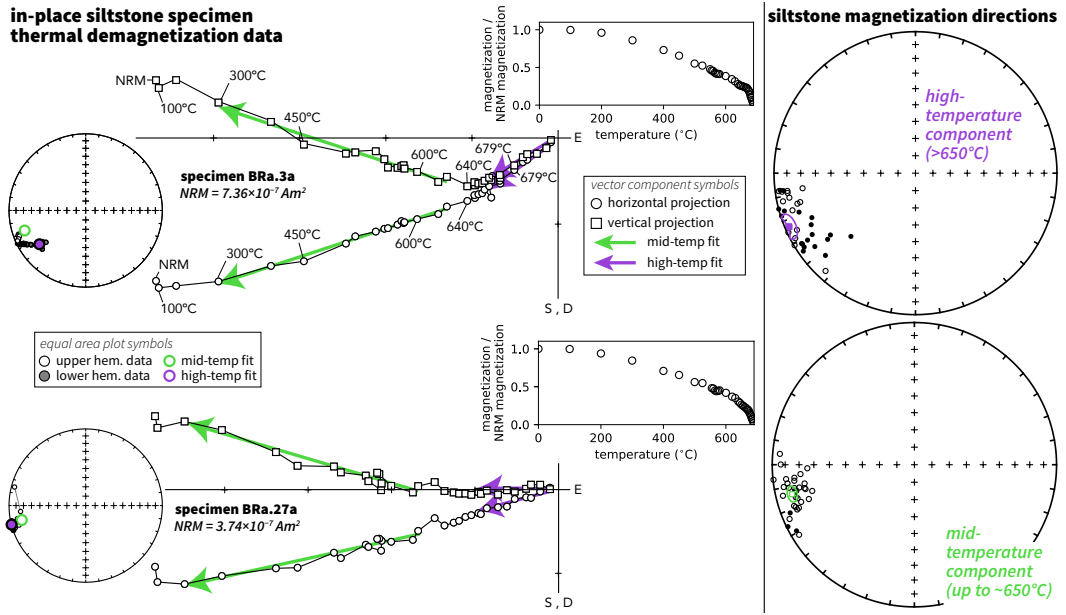


Figure 3. Paleomagnetic data from in-place siltstone beds reveal a mid-temperature component that typically unblocks prior to 655°C and a high-temperature component that typically unblocks between 655°C and 687°C . The direction of the mid-temperature component is shown as purple arrows on the vector component plots and purple circles on the equal area plots while the high-temperature component is shown with green symbols. The mid-temperature component is similar to that removed from the clasts. The high-temperature component is well-grouped and has a distinct direction from the mid-temperature component with lower inclination.

Rock Magnetic and Mössbauer Spectroscopy Results

The paleomagnetic data reveal that there are two distinct populations of remanence carrying magnetic grains within the intraclasts and in-place siltstone with differing ranges of unblocking temperatures. Rock magnetic experiments can elucidate more information about the ferromagnetic mineralogy within the siltstone that is carrying the remanence as well as portions of the magnetic mineralogy that are not stable at room temperature.

Backfield demagnetization curves where the specimens were saturated in a 1.8 T followed by a progressively larger field in the opposite direction were developed on a Princeton Measurements vibrating sample magnetometer at the Institute for Rock Magnetism. Coercivity spectra, the derivative of the backfield curves, were modeled using the Max UnMix software package (Maxbauer, Feinberg, & Fox, 2016; Fig. 4). These spectra can be well fit with two log-normal distributions associated with two populations of grains. One population has a median coercivity of $\sim 300 \text{ mT}$ and a distribution that extends from the lowest to the highest coercivities. The other population has a higher median coercivity of $\sim 1000 \text{ mT}$ and a coercivity distribution that is limited to the high coercivity range. The median coercivity of the high coercivity phase corresponds well with the coercivity of single-domain hematite in the 300 nm to $10 \mu\text{m}$ range (Özdemir & Dunlop, 2014). The spread in coercivity values associated with the lower coercivity population is consistent with the values for hematite from these values down to that associated with finer-grained hematite as the coercivity of hematite becomes progressively lower for grains that are smaller than 300 nm .

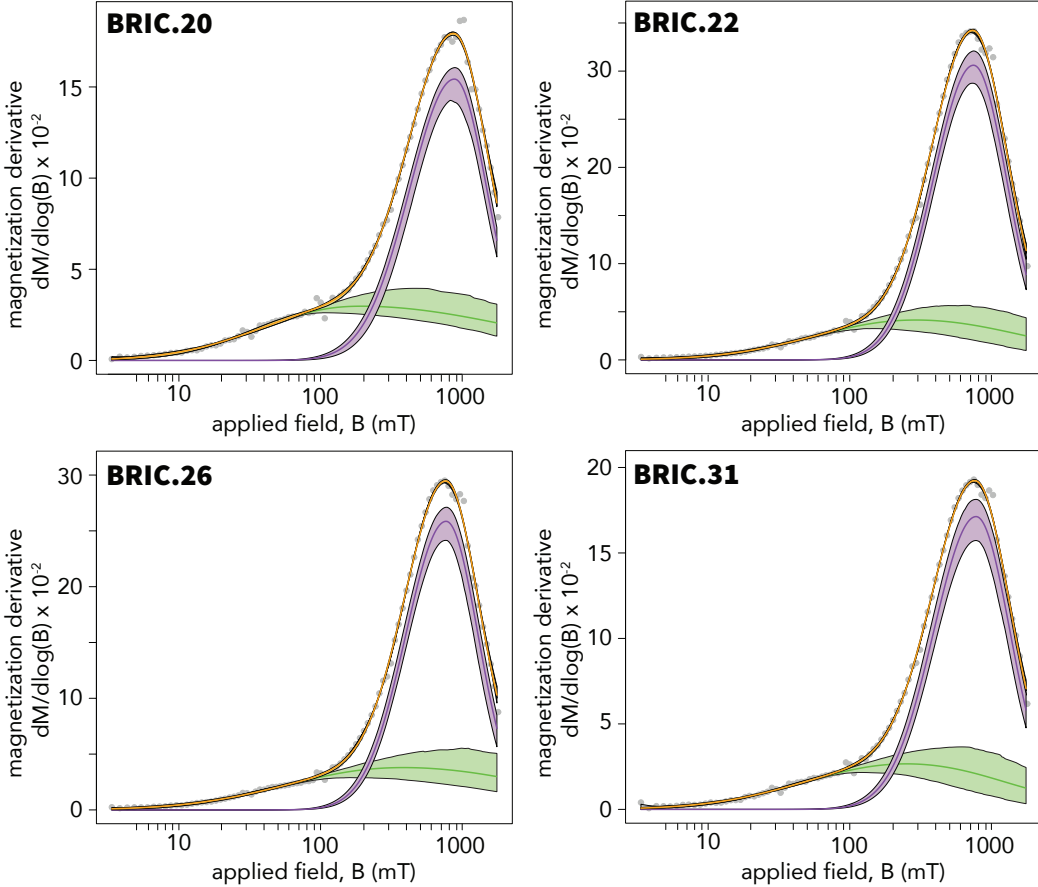


Figure 4. Coercivity spectra developed from backfield demagnetization curves on BRIC intraclast specimens with the points being the data. The data were modeled using log-Gaussian functions implemented with the Max UnMix software package (Maxbauer et al., 2016) with the yellow curve corresponding to the model. The coercivity spectra can be well-explained with two distributions: the higher coercivity distribution in purple and the lower coercivity distribution in green.

The frequency and temperature dependence of magnetic susceptibility was determined through experiments using a Magnetic Properties Measurement System (MPMS) at the Institute for Rock Magnetism. The dependence of susceptibility on both temperature and frequency provides a sensitive and diagnostic means of characterizing magnetic nanoparticles. We observe a frequency dependence of susceptibility that persists from 300 K down to 10 K (Fig. 5). This frequency dependence can be attributed to viscous superparamagnetic grains whose magnetic viscosity has relaxation times comparable to the AC field reversal interval given that it is expressed in the in-phase susceptibility, the out-of-phase susceptibility and the $\pi/2$ law ?. That the frequency dependence extends across the full low-temperature range indicates a broad blocking temperature spectrum of viscous superparamagnetic associated with a wide size distribution of the nanoparticles.

Mössbauer spectra were collected at the Institute for Rock Magnetism on bulk powders of intraclast samples at 300 K and 18 K (Fig. 6). The main feature of these spectra is the magnetically split sextet with a magnetic hyperfine field of about 51.6 T di-

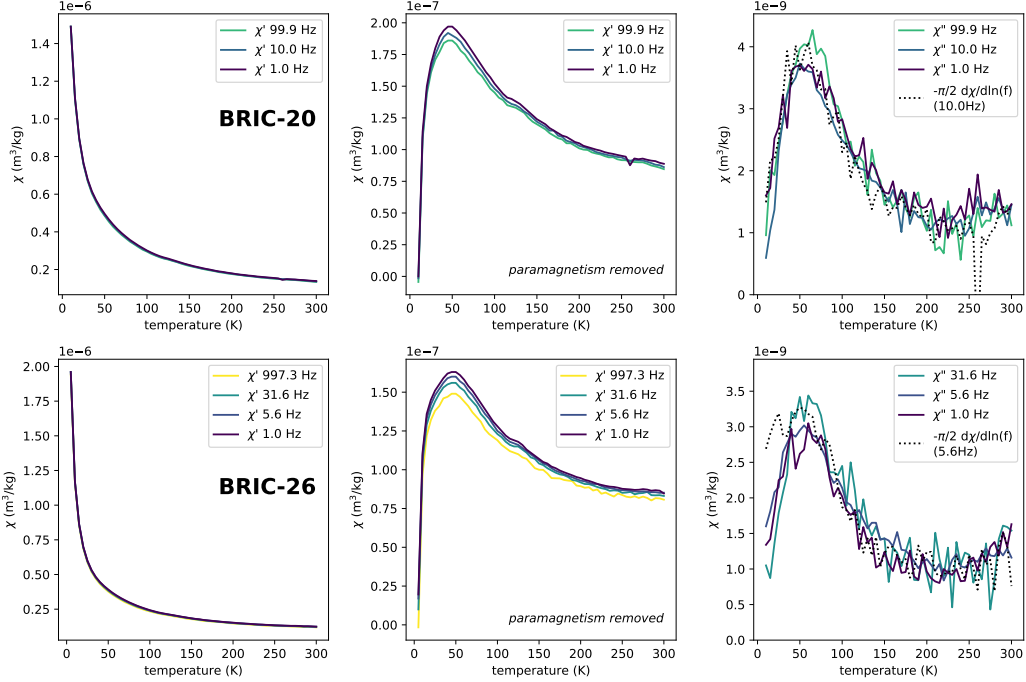


Figure 5. Frequency and temperature dependence of magnetic susceptibility for BRIC-20 and BRIC-22 from 10 to 300 K. The left panels show the in-phase susceptibility which is dominated by the paramagnetic component of the samples. In the middle panels, this paramagnetic component has been removed by creating a Curie-Weiss law model and subtracting it from the in-phase susceptibility data. Strong frequency dependence over the whole temperature range suggests a broad size distribution of nanoparticles (e.g. Jackson & Swanson-Hysell, 2012). The right panels show the out-of-phase (quadrature) susceptibility as well as the $\pi/2$ relationship where $\chi''[\text{viscosity}] = -(\pi/2)(\partial\chi'/\partial\ln(f))$. These data document the presence of viscous superparamagnetic particles.

agnostic of hematite (Dyar, Agresti, Schaefer, Grant, & Sklute, 2006). Modeling of the spectra reveal that the majority of iron within the samples resides within hematite (58% at 300 K and 60% at 18 K). Due to the high-frequency at which Mössbauer spectra are collected, grains that are typically considered to be superparamagnetic at room temperature behave as stable ordered grains. Nevertheless, there is a slight increase in the relative magnitude of the hematite sextet relative to the doublets without hyperfine splitting in the 18 K spectrum that is likely associated with ordering of nanoparticles of hematite.

DISCUSSION

Single-domain hematite grains have high coercivities (>150 mT; Özdemir & Dunlop, 2014) and high unblocking temperatures. As a result, populations of hematite within rocks are stable on long timescales, resistant to overprinting, and therefore attractive for paleomagnetic study. In contrast to magnetite, hematite grains retain stable single-domain behavior in crystals $>1\mu\text{m}$ with the threshold to multidomain behavior occurring when grain diameters exceed $\sim 100\mu\text{m}$ (Kletetschka & Wasilewski, 2002; Özdemir & Dunlop, 2014). Hematite nanoparticles with diameters <30 nm have superparamagnetic behavior wherein thermal fluctuation energy overwhelms the ability of the grain to retain a stable magnetization at Earth surface temperatures (Özdemir & Dunlop, 2014). Hematite

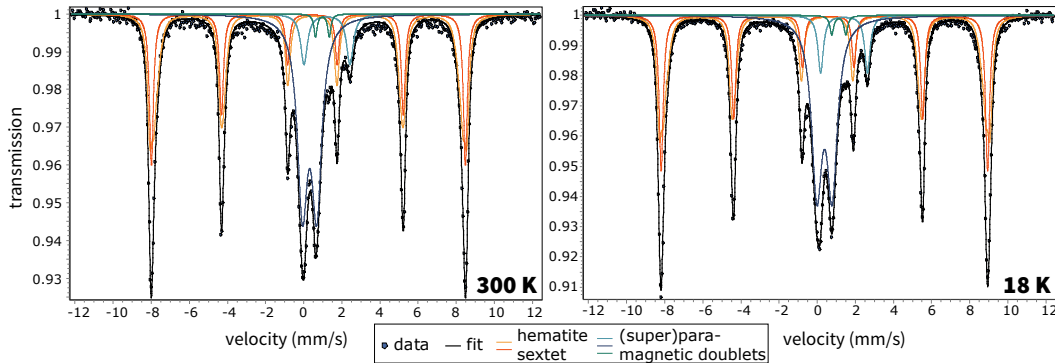


Figure 6. Mössbauer spectra developed at room temperature (300 K) and low temperature (18 K) on a powder of intraclast sample BRIC.22. Data are shown as dots with the black line representing a model fit. The sextet portion of the fit is shown with the red and yellow curves (representing the spread in hyperfine splitting resulting from a natural population) and is diagnostic of hematite. The central peak is comprised of doublets dominated by Fe^{3+} . The relative height of the hematite sextet relative to the central peak is slightly higher in the low temperature experiment likely due to ordering of the smallest hematite nanoparticles.

grains become progressively less influenced by thermal fluctuations as they reach grain sizes of a few hundred nanometers at which point they are stable up to temperatures approaching the Néel temperature of $\sim 685^\circ\text{C}$ (Özdemir & Dunlop, 2014; Swanson-Hysell, Feinberg, Berquó, & Maloof, 2011). As a result, there is a strong relationship between grain volume and unblocking temperature that can be utilized to estimate grain size. A hematite population that is progressively unblocking at thermal demagnetization steps well below the Néel transition temperature, such as the mid-temperature component of the intraclasts, is comprised of grains within the ~ 30 to ~ 400 nm size range. This fine-grain size is consistent with the pigmentary phase observed within the intraclasts (Fig. 1).

Given the directional consistency of the mid-temperature component among the intraclasts, this component must have dominantly formed as a chemical remanent magnetization after the intraclasts were redeposited in the channel. Chemical remanent magnetization acquisition by pigmentary hematite would have occurred as hematite grains grew to sizes above the superparamagnetic to stable single-domain transition resulting in the wide range of unblocking temperatures that is observed. In contrast, given its sharp unblocking temperature close to the Néel temperature, the high-temperature component is dominantly held by hematite grains that are >400 nm such as the silt-sized hematite grains observed petrographically (Fig. 1). The high-temperature remanence component held by these grains was rotated along with the clasts indicating that it is primary and was acquired prior to the redeposition of the cohesive silt clasts. That this component is held by larger grain sizes supports it being a detrital remanent magnetization, rather than a chemical remanent magnetization that formed very early prior to clast erosion.

Oxidation of iron in aqueous environments often proceeds through the formation of fine-grained poorly crystalline ferrihydrite, which transforms to stable crystalline hematite at neutral pH on geologically short timescales (Cudennec & Lecerf, 2006). The broad unblocking temperatures we observe for the chemical remanent magnetization in the Freda intraclasts are similar to those in hematite populations produced through experimental ferrihydrite to hematite conversion (Jiang et al., 2015). The differential unblocking temperature spectra of the two components within the Freda intraclasts provides strong

support for the argument of Jiang et al. (2015) that chemical and detrital remanent magnetization can be distinguished; due to detrital remanence unblocking at the highest temperatures. However, it is also clear from the Freda intraclast data that while the detrital remanent magnetization can be well-isolated at temperatures as low as 650°C (specimen BRIC.31a in Fig. 2), the chemical remanent magnetization thermal unblocking spectra can overlap with that of the detrital remanence and extend up to temperatures closer to the Néel temperature (specimen BRIC.41a in Fig. 2). Therefore, to isolate primary remanence in red beds, best practice should be to proceed with very high resolution thermal demagnetization steps above 600°C, and particularly above 650°C. These intraclast data reveal that directional change at the highest unblocking temperatures provides an effective means to discriminate primary and secondary magnetizations within siltstones of the Freda formation and other red beds. The formation of coarse-grained secondary hematite can occur, particularly in high permeability lithologies and deeply weathered profiles. However, the isolation of primary detrital hematite in >1 billion-year-old siltstones lends confidence to magnetostratigraphic records and paleogeographic interpretations that are based on interpretations of primary magnetization in ancient red beds.

Acknowledgments

This research was supported by the Esper S. Larsen, Jr. Research Fund and the National Science Foundation through grant EAR-1419894. SPS was supported by the Miller Institute for Basic Research in Science. The Wisconsin Department of Natural Resources granted a research and collection permit that enabled sampling within Copper Falls State Park. Oliver Abbitt assisted with field work, Taiyi Wang assisted with paleomagnetic analyses and Tim Teague provided technical support for EBSD analyses. Data are available within the MagIC database and a Github repository associated with this work.

References

- Beck, M. E., Burmester, R. F., & Housen, B. A. (2003, Feb). The red bed controversy revisited: shape analysis of Colorado Plateau units suggests long magnetization times. *Tectonophysics*, 362(1-4), 335–344. Retrieved from [http://dx.doi.org/10.1016/S0040-1951\(02\)00644-3](http://dx.doi.org/10.1016/S0040-1951(02)00644-3) doi: 10.1016/s0040-1951(02)00644-3
- Bilardello, D., & Kodama, K. P. (2010, Mar). Palaeomagnetism and magnetic anisotropy of carboniferous red beds from the maritime provinces of canada: evidence for shallow palaeomagnetic inclinations and implications for north american apparent polar wander. *Geophysical Journal International*, 180(3), 1013–1029. Retrieved from <http://dx.doi.org/10.1111/j.1365-246X.2009.04457.x> doi: 10.1111/j.1365-246x.2009.04457.x
- Butler, R. (1992). *Paleomagnetism: Magnetic domains to geologic terranes*. Blackwell Scientific Publications.
- Cannon, W. F., & Hinze, W. J. (1992, 10 30). Speculations on the origin of the North American Midcontinent rift. *Tectonophysics*, 213(1-2), 49–55. doi: 10.1016/0040-1951(92)90251-Z
- Collinson, D. W. (1965, Feb). Origin of remanent magnetization and initial susceptibility of certain red sandstones. *Geophysical Journal International*, 9(2-3), 203–217. Retrieved from <http://dx.doi.org/10.1111/j.1365-246X.1965.tb02071.x> doi: 10.1111/j.1365-246x.1965.tb02071.x
- Cudennec, Y., & Lecerf, A. (2006, Mar). The transformation of ferrihydrite into goethite or hematite, revisited. *Journal of Solid State Chemistry*, 179(3), 716–722. Retrieved from <http://dx.doi.org/10.1016/j.jssc.2005.11.030> doi: 10.1016/j.jssc.2005.11.030
- DiVenere, V. J., & Opdyke, N. D. (1991). Magnetic polarity stratigraphy in the uppermost mississippian mauch chunk formation, pottsville, penn-

- 347 sylvania. *Geology*, 19(2), 127. Retrieved from [http://dx.doi.org/10.1130/0091-7613\(1991\)019<0127:mfpsitu>2.3.co;2](http://dx.doi.org/10.1130/0091-7613(1991)019<0127:MPSITU>2.3.CO;2) doi: 10.1130/0091-7613(1991)019<0127:mfpsitu>2.3.co;2
- 348 Dyar, M. D., Agresti, D. G., Schaefer, M. W., Grant, C. A., & Sklute, E. C. (2006,
349 May). Mössbauer spectroscopy of earth and planetary materials. *Annual
350 Review of Earth and Planetary Sciences*, 34(1), 83–125. Retrieved from
351 <http://dx.doi.org/10.1146/annurev.earth.34.031405.125049> doi:
352 10.1146/annurev.earth.34.031405.125049
- 353 Elmore, R. D., & Van der Voo, R. (1982). Origin of hematite and its associated re-
354 manence in the Copper Harbor Conglomerate (Keweenawan), upper Michigan.
355 *J. Geophys. Res.*, 87(B13), 10918–10928. doi: 10.1029/JB087iB13p10918
- 356 Fairchild, L. M., Swanson-Hysell, N. L., Ramezani, J., Sprain, C. J., & Bowring,
357 S. A. (2017, 01). The end of Midcontinent Rift magmatism and the paleo-
358 geography of Laurentia. *Lithosphere*, 9(1), 117–133. Retrieved from <http://lithosphere.gsapubs.org/content/early/2017/01/05/L580.1.abstract>
359 doi: 10.1130/L580.1
- 360 Henry, S., Mauk, F., & Van der Voo, R. (1977). Paleomagnetism of the upper Ke-
361 weenawan sediments: Nonesuch Shale and Freda Sandstone. *Canadian Journal
362 of Earth Science*, 14, 1128–1138. doi: 10.1139/e77-103
- 363 Hutchinson, D., White, R., Cannon, W., & Schulz, K. (1990). Keweenaw hot spot:
364 Geophysical evidence for a 1.1 Ga mantle plume beneath the Midcontinent
365 Rift System. *Journal of Geophysical Research: Solid Earth*, 95(B7), 10869–
366 10884. doi: 10.1029/jb095ib07p10869
- 367 Jackson, M., & Swanson-Hysell, N. (2012). Rock magnetism of remagnetized car-
368 bonate rocks: Another look. In R. Elmore (Ed.), *Remagnetization and chemi-
369 cal alteration of sedimentary rocks* (Vol. 371). Geological Society London, Spe-
370 cial Publications. doi: 10.1144/SP371.3
- 371 Jiang, Z., Liu, Q., Dekkers, M. J., Tauxe, L., Qin, H., Barrón, V., & Torrent, J.
372 (2015, Oct). Acquisition of chemical remanent magnetization during ex-
373 perimental ferrihydrite–hematite conversion in earth-like magnetic field—
374 implications for paleomagnetic studies of red beds. *Earth and Planetary
375 Science Letters*, 428, 1–10. Retrieved from <http://dx.doi.org/10.1016/j.epsl.2015.07.024> doi: 10.1016/j.epsl.2015.07.024
- 376 Kirschvink, J. (1980). The least-squares line and plane and the analysis of paleomag-
377 netic data. *Geophysical Journal of the Royal Astronomical Society*, 62(3), 699–
378 718. doi: 10.1111/j.1365-246x.1980.tb02601.x
- 379 Kletetschka, G., & Wasilewski, P. J. (2002). Grain size limit for SD hematite.
380 *Physics of the Earth and Planetary Interiors*, 129, 173–179. doi: 10.1016/S0031-9201(01)00271-0
- 381 Larson, E. E., & Walker, T. R. (1982, Jun). A rock magnetic study of the lower
382 massive sandstone, Moenkopi Formation (Triassic), Gray Mountain Area,
383 Arizona. *Journal of Geophysical Research: Solid Earth*, 87(B6), 4819–
384 4836. Retrieved from <http://dx.doi.org/10.1029/JB087iB06p04819> doi:
385 10.1029/jb087ib06p04819
- 386 Maxbauer, D. P., Feinberg, J. M., & Fox, D. L. (2016, Oct). MAX UnMix: A web
387 application for unmixing magnetic coercivity distributions. *Computers and
388 Geosciences*, 95, 140–145. Retrieved from <http://dx.doi.org/10.1016/j.cageo.2016.07.009> doi: 10.1016/j.cageo.2016.07.009
- 389 Ojakangas, R. W., Morey, G. B., & Green, J. C. (2001, 6 1). The Mesoproterozoic
390 Midcontinent Rift System, Lake Superior Region, USA. *Sedimentary Geology*,
391 141–142, 421–442. doi: 10.1016/s0037-0738(01)00085-9
- 392 Özdemir, Ö., & Dunlop, D. J. (2006). Magnetic memory and coupling between spin-
393 canted and defect magnetism in hematite. *J. Geophys. Res.*, 111(B12). doi: 10
394 .1029/2006JB004555
- 395 Özdemir, Ö., & Dunlop, D. J. (2014). Hysteresis and coercivity of hematite. *Jour-*

- 402 *nal of Geophysical Research: Solid Earth*, 119(4), 2582–2594. Retrieved from
 403 <http://dx.doi.org/10.1002/2013JB010739> doi: 10.1002/2013JB010739

404 Purucker, M. E., Elston, D. P., & Shoemaker, E. M. (1980). Early acquisition
 405 of characteristic magnetization in red beds of the Moenkopi Formation (Tri-
 406 assic), Gray Mountain, Arizona. *Journal of Geophysical Research*, 85(B2),
 407 997. Retrieved from <http://dx.doi.org/10.1029/JB085iB02p00997> doi:
 408 10.1029/jb085ib02p00997

409 Swanson-Hysell, N. L., Feinberg, J. M., Berquó, T. S., & Maloof, A. C. (2011, 5).
 410 Self-reversed magnetization held by martite in basalt flows from the 1.1-billion-
 411 year-old Keweenawan rift, Canada. *Earth and Planetary Science Letters*,
 412 305(1-2), 171–184. doi: 10.1016/j.epsl.2011.02.053

413 Tauxe, L., Kent, D. V., & Opdyke, N. D. (1980). Magnetic components contributing
 414 to the NRM of Middle Siwalik red beds. *Earth and Planetary Science Letters*,
 415 47, 279–284. (10.1016/0012-821X(80)90044-8)

416 Tauxe, L., Shaar, R., Jonestrask, L., Swanson-Hysell, N., Minnett, R., Koppers,
 417 A., ... Fairchild, L. (2016). PmagPy: Software package for paleomag-
 418 netic data analysis and a bridge to the Magnetics Information Consor-
 419 tium (MagIC) Database. *Geochemistry, Geophysics, Geosystems*. doi:
 420 10.1002/2016GC006307

421 Van Der Voo, R., & Torsvik, T. H. (2012, 01). The history of remagnetization of
 422 sedimentary rocks: deceptions, developments and discoveries. *Geological Soci-
 423 ety, London, Special Publications*, 371(1), 23–53. doi: 10.1144/SP371.2

424 Van Houten, F. B. (1968). Iron oxides in red beds. *Geological Society of Amer-
 425 ica Bulletin*, 79(4), 399. Retrieved from [http://dx.doi.org/10.1130/0016-7606\(1968\)79\[399:
 426 ioirb\]2.0.co;2](http://dx.doi.org/10.1130/0016-7606(1968)79[399:IOIRB]2.0.CO;2) doi: 10.1130/0016-7606(1968)79[399:
 427 ioirb]2.0.co;2